

Raman scattering study of electron-doped $\text{Pr}_x\text{Ca}_{1-x}\text{Fe}_2\text{As}_2$ superconductors

A. P. Litvinchuk,^{1,*} Bing Lv,¹ and C. W. Chu^{1,2}

¹Texas Center for Superconductivity and Department of Physics, University of Houston, Texas 77204-5002, USA

²Lawrence Berkeley National Laboratory, Berkeley, California 94720, USA

(Received 11 July 2011; published 14 September 2011)

Temperature-dependent polarized Raman spectra of electron-doped superconducting $\text{Pr}_x\text{Ca}_{1-x}\text{Fe}_2\text{As}_2$ ($x \approx 0.12$) single crystals are reported. All four even-parity phonons allowed by symmetry are identified. The phonon mode of B_{1g} symmetry at 222 cm^{-1} , which is associated with the c -axis motion of Fe ions, is found to exhibit an anomalous frequency hardening at low temperatures, that signals nonvanishing electron-phonon coupling in the superconducting state and implies that the superconducting gap magnitude $2\Delta_c < 27\text{ meV}$.

DOI: [10.1103/PhysRevB.84.092504](https://doi.org/10.1103/PhysRevB.84.092504)

PACS number(s): 74.70.Xa, 74.25.Kc, 63.20.kk, 78.30.-j

Since the first reports on superconductivity in iron-arsenide-based oxypnictides $\text{LaF}_x\text{O}_{1-x}\text{FeAs}$,^{1,2} a number of closely related compounds have been discovered³⁻⁵ and there is a continuing effort to optimize their superconducting properties and raise the superconductivity transition temperature. It is well understood that, as for other superconductors, one of the key factors in achieving this goal is proper material doping. As far as $Ae\text{Fe}_2\text{As}_2$ (where Ae is an alkali earth element) systems are concerned, until recently the highest superconducting temperature on record was at $T_c = 38\text{ K}$ for the $\text{K}_x\text{Ba}_{1-x}\text{Fe}_2\text{As}_2$ system,^{4,5} where optimum doping takes place at $x \approx 0.4$. In that case, indirect hole doping of FeAs layers was realized.

Several attempts have been reported to introduce electron doping into $Ae\text{Fe}_2\text{As}_2$ systems in a search for materials with higher T_c 's. Muraba *et al.*⁶ observed superconductivity up to $T_c = 22\text{ K}$ in the case of La^{3+} -for- Sr^{2+} substitution. Theoretical calculations show clear differences between hole- and electron-doped systems⁷ and predict that superconductivity can sustain higher hole than electron doping.⁸ Despite this fact, it was found recently that the superconducting transition temperature T_c reaches 45 K (under pressure) in the case of La^{3+} -for- Ca^{2+} substitution,⁹⁻¹¹ and as high as 49 K for Pr^{3+} indirect doping, as shown by resistive, magnetic, and thermoelectric measurements.¹² It is unclear, however, whether the superconducting transition observed is bulk⁹ or nonbulk¹² due to interfacial or filamentary superconductivity. Interfacial or filamentary superconductivity has been suggested to lead to an enhanced T_c .¹³

In this communication we report the results of a Raman scattering study of Pr^{3+} -doped CaFe_2As_2 single crystals. Even though the phonons themselves and the strength of electron-phonon interactions are not sufficient to explain the rather high T_c in this class of materials,¹⁴ we focus on the phonon spectra and lattice vibrations, which, due to their coupling to the electronic states, may shed light on the origin of superconductivity and the details of the interplay among lattice, charge, and spin degrees of freedom. The samples studied here were CaFe_2As_2 single crystals doped with Pr at the level $x \approx 0.12$. They showed two superconducting transitions, at $T_c = 49\text{ K}$ and $T_c = 21\text{ K}$. The preparation technique and characterization of single crystals by x-ray diffraction, transport, and magnetic susceptibility measurements have been reported in Ref. 12.

Raman scattering measurements were performed with a triple Horiba Jobin Yvon T64000 spectrometer, equipped with an optical microscope and liquid-nitrogen-cooled CCD detector. Samples were mounted on the cold finger of a helium flow optical cryostat and the temperature was controlled within 0.1 K . A He-Ne laser ($\lambda_{\text{las}} = 638.2\text{ nm}$) was used as the excitation source and the power density did not exceed 10^4 W/cm^2 , in order to minimize heating of the sample.

$Ae\text{Fe}_2\text{As}_2$ compounds crystallize in the tetragonal ThCr_2Si_2 -type structure¹⁵ within the space group $I4/mmm$ and their vibrational spectra are well understood.¹⁶ Model calculations (density functional theory as well as shell model) reproduce experimental phonon frequencies rather well and provide information on displacement patterns for lattice eigenmodes. The alkaline earth element does not contribute to any of the Raman-active modes, as it occupies a centrosymmetric position within the lattice. Fe and As ions contribute B_{1g} and A_{1g} modes, respectively, which correspond to atomic displacements along the c axis. ab -plane displacements of Fe and As produce two E_g modes, which involve motion of both ions and are therefore strongly mixed.¹⁶ The experimental frequencies of the Raman-active modes (at room temperature) are $114, 182, 204, \text{ and } 264\text{ cm}^{-1}$ ($E_g, A_{1g}, B_{1g}, \text{ and } E_g$, respectively) for undoped SrFe_2As_2 ; $124, 209, \text{ and } 264\text{ cm}^{-1}$ (the A_{1g} mode was not observed from the ab surfaces of the crystals) for BaFe_2As_2 ;¹⁷ and $189 \text{ and } 211\text{ cm}^{-1}$ (A_{1g} and B_{1g}) for CaFe_2As_2 .¹⁸ Thus, for the reason given above, the mode frequencies do not vary strongly upon replacement of the alkaline earth element in the structure.

Figure 1 shows room-temperature Raman scattering spectra of Pr-doped CaFe_2As_2 for different scattering geometries. The spectra were taken from the edge of a thin crystal with a well-developed (a - b) surface, so that the light was propagating in the ab plane. This geometry allowed us to measure spectra in the back-scattering configuration with the light polarized either along the z axis or perpendicular to it. Knowing that the A_{1g} phonon is strong in the (zz) scattering configuration,¹⁶ we readily identified all four modes allowed by symmetry in $\text{Pr}_x\text{Ca}_{1-x}\text{Fe}_2\text{As}_2$: $112, 182, 216, \text{ and } 268\text{ cm}^{-1}$ ($E_g, A_{1g}, B_{1g}, \text{ and } E_g$, respectively).

Further, we performed temperature-dependence measurements using a crystal, which allowed simultaneous observation of A_{1g} and B_{1g} modes. Due to the weak scattering efficiency, an acquisition time of $60\text{--}100\text{ min}$ per spectrum was required.

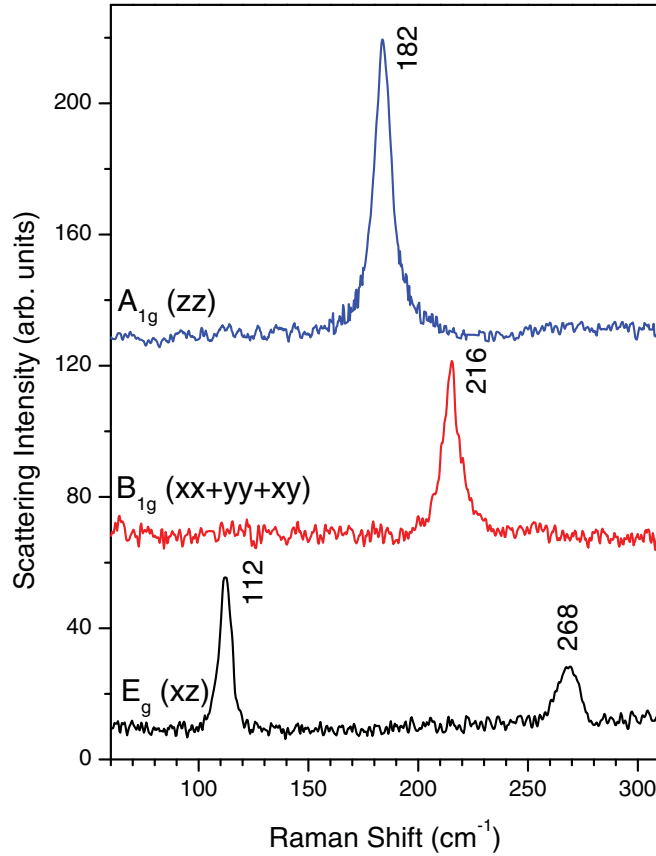


FIG. 1. (Color online) Raman spectra of $\text{Pr}_x\text{Ca}_{1-x}\text{Fe}_2\text{As}_2$ for selected scattering geometries taken at room temperature. Allowed mode symmetries are also listed.

Spectra for selected temperatures are displayed in Fig. 2, and the results of their analysis are summarized in Fig. 3. We note that the instrumental resolution of the spectrometer was small (1.6 cm^{-1}) in comparison to measured phonon linewidths, so that any correction due to deconvolution (below 0.2 cm^{-1}) are neglected.

The temperature dependence of the linewidth (full width at half-maximum) of the modes appears to be very unusual. Each of the modes exhibits changes of only about 1 cm^{-1} between 5 and 200 K, and the low-temperature values of the width are 6.4 and 8.7 cm^{-1} [Figs. 3(b) and 3(d) for B_{1g} and A_{1g} modes, respectively]. This implies that, apart from conventional anharmonic phonon decay processes, which typically govern line broadening as a function of temperature for insulating and semiconducting materials, some other processes are involved.

Indeed, phonon anharmonicity leads to the following temperature dependence of the linewidth Γ and mode frequency ω :^{19–21}

$$\Gamma(T) = \gamma + \Gamma_0 \left(1 + \frac{2}{e^{\hbar\omega_0/2k_B T} - 1} \right), \quad (1)$$

$$\omega(T) = \omega_0 - C \left(1 + \frac{2}{e^{\hbar\omega_0/2k_B T} - 1} \right), \quad (2)$$

where $\hbar\omega_0$ is the phonon frequency, k_B is the Boltzmann constant, and C is a constant. For insulators and semiconductors Γ_0 is the only parameter needed to adequately describe the temperature dependence of the linewidth (so that $\gamma = 0$). In the

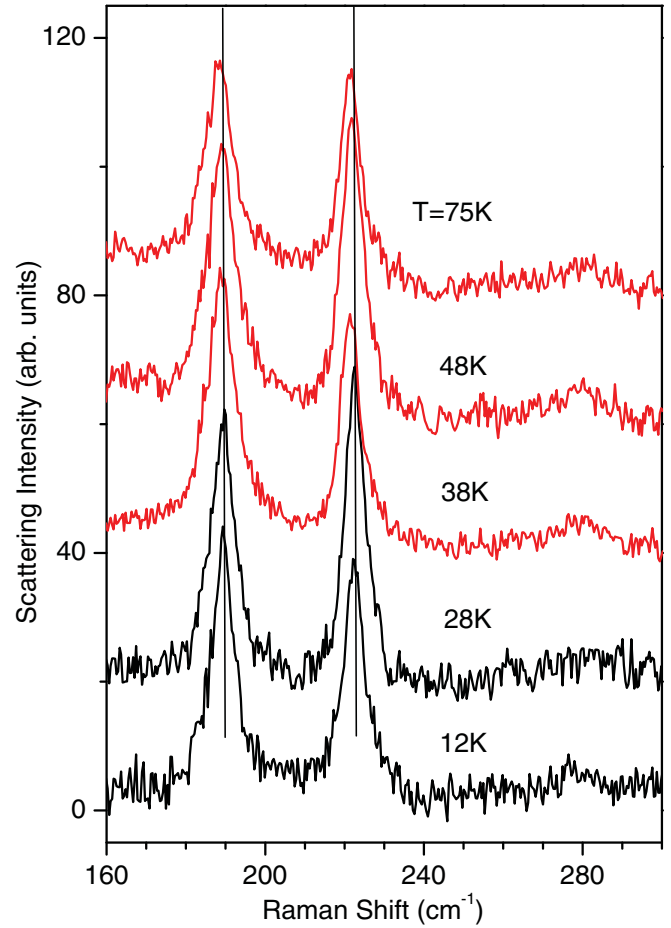


FIG. 2. (Color online) Temperature-dependent Raman scattering spectra of $\text{Pr}_x\text{Ca}_{1-x}\text{Fe}_2\text{As}_2$. Vertical lines mark the low-temperature position of the lines.

case of a crystal with defects (impurities, structural imperfections, etc.), an additional temperature-independent component of the linewidth γ might be required. Naturally, phonon interactions with other excitations (electrons in conducting materials, e.g.), which open additional channels for phonon decay, will influence the phonon lifetime and contribute to the phonon linewidth $\Gamma(T)$.²² This is in fact the phenomenon that could be used to monitor features of electronic spectra such as gap opening in superconductors^{23–25} and spin excitations of superconductors and/or magnetically ordered systems.^{26–28}

Solid lines in Figs. 3(b) and 3(d) are plotted following Eq. (1). The fit of the temperature-dependent linewidth yields $\gamma \gg \Gamma_0$ for both B_{1g} (6.0 vs 0.4 cm^{-1}) and A_{1g} (8.3 vs 0.4 cm^{-1}) modes. Small values of Γ_0 with respect to the γ clearly signal that lattice anharmonicity is not a dominant mechanism of the phonon decay in the material under investigation. Thus, the phonon coupling to electrons in the conducting $\text{Pr}_x\text{Ca}_{1-x}\text{Fe}_2\text{As}_2$ governs the T dependence of the linewidth over the whole temperature range. We also note that the phonon linewidths observed for Pr-doped CaFe_2As_2 , which are shown in Fig. 3, are larger compared to those reported by Choi *et al.* in Ref. 18 for an undoped parent CaFe_2As_2 compound (about 4.2 and 4.5 cm^{-1} for A_{1g} and B_{1g} modes, respectively). This could be due to modification by Pr doping

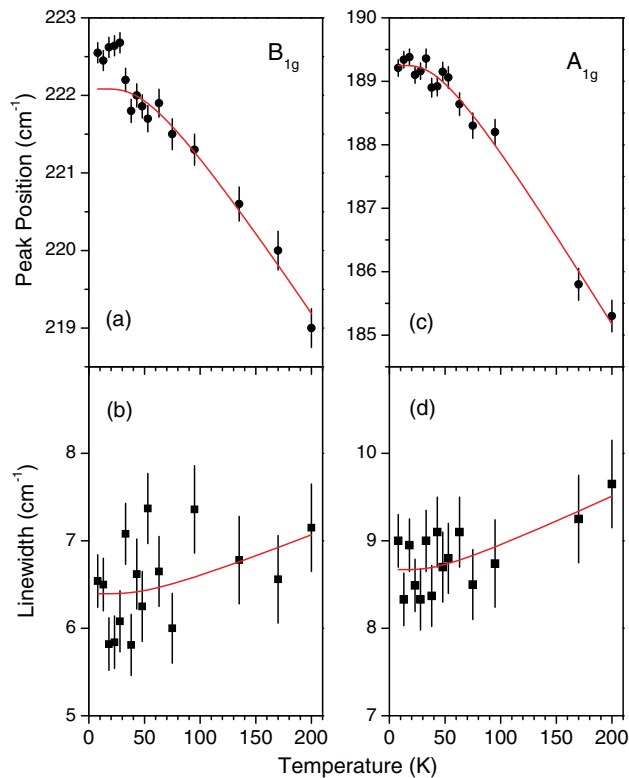


FIG. 3. (Color online) Position (a, c) and linewidth (b, d) of A_{1g} and B_{1g} modes as a function of temperature. Solid lines show the expected behavior due to anharmonic phonon decay (see text). Note the anomalous B_{1g} mode frequency hardening at low temperatures.

of the electronic states, to which phonons couple, but also, at least partly, due to substitutional disorder.

Next, using Eq. (2), the predicted anharmonic behavior of mode frequencies is shown by solid lines in Figs. 3(a)

and 3(c). It well describes the temperature dependence of the A_{1g} mode. The B_{1g} mode at 222 cm^{-1} exhibits, however, clear deviation from the expected behavior below 38 K. This implies redistribution upon cooling of electronic states, to which this mode couples, and is a consequence of a gap opening. Phonon hardening implies that the mode frequency exceeds the gap magnitude $2\Delta_c$.^{23,24}

The fact that the B_{1g} phonon mode, but not the A_{1g} mode, exhibits specific features upon entering the superconducting state in electron-doped $\text{Pr}_x\text{Ca}_{1-x}\text{Fe}_2\text{As}_2$ is not surprising in view of recent findings in theoretical band structure calculations and experimental analysis of symmetry-dependent electron-phonon coupling and electronic inelastic light scattering.^{29,30} Indeed, the A_{1g} scattering channel is shown to probe Brillouin center hole Fermi sheets, B_{2g} (E_g in the tetragonal notations) is maximal at the edges of the Brillouin zone ($\pi/2, \pi/2$), where there are no Fermi sheets, and the B_{1g} channel couples to the *electronic* pockets of the Fermi surface. This could be the reason for the observed B_{1g} -symmetry phonon anomalies in electron-doped $\text{Pr}_x\text{Ca}_{1-x}\text{Fe}_2\text{As}_2$ superconductors, which were not detected earlier in hole-doped $\text{K}_x\text{Sr}_{1-x}\text{Fe}_2\text{As}_2$.¹⁶

In conclusion, all four Raman-active phonons in $\text{Pr}_x\text{Ca}_{1-x}\text{Fe}_2\text{As}_2$ ($x \approx 0.12$) have been observed experimentally. Anomalous B_{1g} mode hardening is observed upon entering the superconducting state, which is associated with the opening of the superconducting gap below the phonon mode frequency (222 cm^{-1}), so that the gap magnitude $2\Delta_c < 27\text{ meV}$; i.e., $2\Delta_c < 6.3k_B T_c$ for critical temperature $T_c = 49\text{ K}$.

This work is supported in part by the T.L.L. Temple Foundation, the J. J. and R. Moores Endowment, the State of Texas through TCSUH, the USAF Office of Scientific Research, and the LBNL through the USDOE. Critical reading of the manuscript by M.N. Iliiev is greatly appreciated.

*alexander.litvinchuk@mail.uh.edu

¹Y. Kamihara, T. Watanabe, M. Hirano, and H. Hosono, *J. Am. Chem. Soc.* **130**, 3296 (2008).

²H. Takahashi, K. Igawa, K. Arii, Y. Kamihara, M. Hirano, and H. Hosono, *Nature* **453**, 376 (2008).

³J. H. Tapp, Z. Tang, Bing Lv, K. Sasmal, B. Lorenz, P. C. W. Chu, and A. M. Guloy, *Phys. Rev. B* **78**, 060505(R) (2008).

⁴M. Rotter, M. Tegel, and D. Johrendt, *Phys. Rev. Lett.* **101**, 107006 (2008).

⁵K. Sasmal, B. Lv, B. Lorenz, A. M. Guloy, F. Chen, Y.-Y. Xue, and C. W. Chu, *Phys. Rev. Lett.* **101**, 107007 (2008).

⁶Y. Muraba, S. Matsuishi, S.-W. Kim, T. Atou, O. Fukunaga, and H. Hosono, *Phys. Rev. B* **82**, 180512 (2010).

⁷I. I. Mazin, D. J. Singh, M. D. Johannes, and M. H. Du, *Phys. Rev. Lett.* **101**, 057003 (2008).

⁸H. Ikeda, R. Arita, and J. Kuneš, *Phys. Rev. B* **81**, 054502 (2010).

⁹Z. Gao, Y. Qi, L. Wang, D. Wang, X. Zhang, C. Yao, C. Wang, and Y. Ma, *EPL* **95**, 67002 (2011).

¹⁰Y. Qi, Z. Gao, L. Wang, D. Wang, X. Zhang, C. Yao, C. Wang, C. Wang, and Y. Ma, e-print [arXiv:1106.4208](https://arxiv.org/abs/1106.4208) (unpublished).

¹¹S. K. Goh, L. E. Klintberg, J. M. Silver, F. M. Grosche, S. R. Saha, T. Drye, J. Paglione, and M. Sutherland, e-print [arXiv:1107.0689](https://arxiv.org/abs/1107.0689) (unpublished).

¹²Bing Lv, L. Z. Deng, M. Gooch, F. Y. Wei, Y. Y. Sun, J. Meen, Y.-Y. Xue, B. Lorenz, and C. W. Chu, *Proc. Nat. Acad. Sci.* (2011), in press.

¹³D. Allender, J. Bray, and J. Bardeen, *Phys. Rev. B* **7**, 1020 (1973).

¹⁴R. H. Liu, T. Wu, G. Wu, H. Chen, X. F. Wang, Y. L. Xie, J. J. Ying, Y. J. Yan, Q. J. Li, B. C. Shi, W. S. Chu, Z. Y. Wu, and X. H. Chen, *Nature* **459**, 64 (2009).

¹⁵S. Rozsa and H. U. Schuster, *Z. Naturforsch. B* **36**, 1668 (1981).

¹⁶A. P. Litvinchuk, V. G. Hadjiev, M. N. Iliiev, Bing Lv, A. M. Guloy, and C. W. Chu, *Phys. Rev. B* **78**, 060503(R) (2008).

¹⁷L. Chauvierre, Y. Gallais, M. Cazayous, A. Sacuto, M. A. Measson, D. Colson, and A. Forget, *Phys. Rev. B* **80**, 094504 (2009).

¹⁸K.-Y. Choi, D. Wulferding, P. Lemmens, N. Ni, S. L. Budko, and P. C. Canfield, *Phys. Rev. B* **78**, 212503 (2008).

¹⁹A. A. Maradudin, P. A. Flinn, and R. A. Coldwellhorsfall, *Ann. Phys.* **15**, 333 (1961).

- ²⁰A. A. Maradudin, P. A. Flinn, and R. A. Coldwellhorsfall, *Ann. Phys.* **15**, 360 (1961).
- ²¹M. Balkanski, R. F. Wallis, and E. Haro, *Phys. Rev. B* **28**, 1928 (1983).
- ²²M. Cardona and I. P. Ipatova, in *Elementary Excitations in Solids*, edited by J. L. Birman, C. Sébenne, and R. F. Wallis (Elsevier, Amsterdam, 1992), p. 237.
- ²³R. Zeyher and A. Zwicknagl, *Z. Phys. B* **78**, 175 (1990).
- ²⁴B. Friedl, C. Thomsen, and M. Cardona, *Phys. Rev. Lett.* **65**, 915 (1990).
- ²⁵A. P. Litvinchuk, C. Thomsen, and M. Cardona, *Solid State Commun.* **80**, 257 (1991).
- ²⁶A. P. Litvinchuk, C. Thomsen, and M. Cardona, *Solid State Commun.* **83**, 343 (1992).
- ²⁷M. N. Iliev, A. P. Litvinchuk, H.-G. Lee, C. W. Chu, A. Barry, and J. M. D. Coey, *Phys. Rev. B* **60**, 33 (1999).
- ²⁸J. Cao, L. I. Vergara, J. L. Musfeldt, A. P. Litvinchuk, Y. J. Wang, S. Park, and S.-W. Cheong, *Phys. Rev. Lett.* **100**, 177205 (2008).
- ²⁹B. Muschler, W. Prestel, R. Hackl, T. P. Devereaux, J. G. Analytis, J.-H. Chu, and I. R. Fisher, *Phys. Rev. B* **80**, 180510(R) (2009).
- ³⁰I. I. Mazin, T. P. Devereaux, J. G. Analytis, J.-H. Chu, I. R. Fisher, B. Muschler, and R. Hackl, *Phys. Rev. B* **82**, 180502(R) (2010).